Research Article: Open Access

DOI: 10.35840/2631-5041/1707

VIBGYOR ePress

International Journal of
Electronics and Device Physics

High-Gain Multi-Layer Antenna Using Metasurface for Application in Terahertz Communication Systems

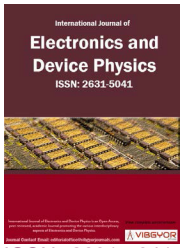

ISSN: 2631-5041

Farzad Khajeh-Khalili and ***Yasaman Dohni-Zadeh***

Electrical Department, Kian Institute of Higher Education, Iran

Abstract

In this paper, a novel high-gain multi-layer antenna is designed for use in terahertz communication systems. The frequency range covered by this antenna is 8-13 THz. To improve the antenna's gain, a proposed rectangular metasurface structure environment has been used. To strengthen and connect the layers, several plastic bases have been used, which do not have a destructive effect on the antenna's radiation pattern. The use of the proposed rectangular metasurface structure medium has increased the gain by more than 10.5 dB compared to the conventional antenna. The maximum gain is 14.7 dB at 12 THz. The final dimensions of this antenna are 24 × 28 × 21.6 mm^3 at 12 THz.

Keywords

Antenna, Metasurface, High-Gian, Terahertz, Multi-Layer

Introduction

The antenna is one of the most important components in designing telecommunication systems to transmit electromagnetic waves or information between transmitters and receivers [1]. From the first time that the antennas were introduced, until now, a variety of antenna structures have been introduced and fabricated. Dipole wired antennas, aperture antenna, horns, and microstrip antennas are among the famous antenna types [2]. Methods of improving the performance of microstrip antennas include the design of array structure [3], the use of special materials such as graphene [4], the employ of metamaterials, metasurfaces, and electromagnetic bandgaps (EBG) [5-7], substrate integrated waveguide (SIW) [8], ridge gap waveguide (RGW) [9] technologies.

Today, it is important to note that the microwave frequency band is no longer popular due to increased demand for higher-rate telecommunications systems and the need for very low data transfer delays [10]. However, the terahertz frequency band is widely used. The high data rate, less interference between signals, as well as increased security and reliability of telecommunications networks, are the advantages of these frequencies [10].

Therefore, in recent years, terahertz antennas have rarely been introduced [11-13]. It should be noted that despite the above benefits, operating in this frequency band also has limitations. For example, many of the above methods, cannot be used to improve the performance of antennas. But

***Corresponding author:** *Dr. Farzad Khajeh-Khalili, Assistant Professor and Head of Electrical Engineering Department, Kian Institute of Higher Education, Shahin Shahr, Isfahan, Iran*

Accepted: October 29, 2020; **Published:** October 31, 2020

Citation: Khajeh-Khalili F, Dohni-Zadeh Y (2020) High-Gain Multi-Layer Antenna Using Metasurface for Application in Terahertz Communication Systems. Int J Electron Device Phys 4:007

metamaterial and metasurface structures in millimeter-wave and terahertz frequency bands, are an efficient tool [14]. Most of the authors' work in recent years has been the design of metamaterial-based antennas and components [14-19].Very recently, in [17], the authors have improved the gain of a microstrip antenna in the millimeter-wave frequencies by more than 11.5 dB, compared to the antenna without any metamaterial structures. The idea now is to design an improved terahertz antenna with improved performance by metasurface technology. In the following, several papers related to the concepts of metamaterial and metasurface are reviewed. It should be noted that metasurfaces are a special case of the metamaterial concept. In the design of metasurface structures, unit-cells with simple structures and in large numbers are usually adjacent to each other and create a metal surface parallel to the dielectric substrate layer in the design of the antenna or other components. However, for the design of metamaterial structures, it is not necessary to be flat. Metamaterial structures can be placed at any angle in antennas. Negative permittivity or permeability parameters in the operating frequency band are among the metamaterial conditions of an environment.

In [19], for the first time, the concept of metamaterial was introduced. But thirty years after the publication of this paper, a sample of artificial metamaterial structures was designed [20]. In these structures, split ring resonators (SRRs) were used to realize the negative permeability and complementary SRRs (CSRRs) were used to realize the negative permittivity. After this work, many examples of metamaterial structures were introduced, with wide bandwidth [21], small dimensions [22], usability in antennas with dual polarization [23], and so on. It should be noted that this issue is still of interest to researchers. But a lot of research has been done on metasurface structures as well [24-28]. In [24], using metasurface structures, a high-isolation two ports antenna in the frequency band of 5.8 GHz to 5.9 GHz is introduced. With employing the metasurfaces, the mutual coupling has reduced by more than 8 dB at 5.8 GHz. In [28], a wideband metasurface antenna with quad-polarization reconfiguration ability is presented. In this work, due to the use of metasurface structures in the central frequency of 5.6 GHz, the gain is more than 9 dBi. Although the performance of this antenna is good, but the large size is its most important drawback. After reference [24], the utilize of metasurface structures in the design of antennas, many researches have been done. But the interesting thing is that very little research has been done to improve the performance of microstrip antennas at terahertz frequencies using metasurfaces. This is one of the most important contributions and also is our motivation for the design of this antenna introduced in this paper.

In this paper, a high-gain multi-layer microstrip antenna using rectangular metasurface structure (RMS) at 8-13 THz for application in terahertz communication systems is proposed. To prove the efficiency of the proposed method, two well-known and full-wave CST Microwave Studio 2019 and HFSSv15 simulators have been used. There is a very good match between the results. Maximum realized gain is 14.7 dB which is 10.6 dB higher than the conventional antenna without the RMS medium at 12 THz. Final dimensions of the proposed antenna are 24 × 28 × 21.6 mm^3 at 12 THz. Also, to better prove the designs procedure, several optimizations as the parametric reports have been done with the mentioned simulators.

Antenna and Rms Design

Proposed RMS and discussion

As mentioned in the previous section, the performance of the proposed terahertz antenna is enhanced by RMSs. The layer containing the proposed RMS is shown in Figure 1a. The rectangular-shaped cell is also shown in Figure 1a. Note that each RMS cell contains four square-shaped metal sections. The dimensions of each section are 0.36 mm^2 at 12 THz. In order to prove the capability of this structure, according to the simulation conditions provided in reference [14], the insertion loss parameter (S_{21}) of this structure has been calculated. Note that the dielectric used is made of RT6010LM dielectric substrate with relative permittivity of 10.7, tan δ = 0.0023, and thickness of 1 mm. In all simulations, CST Microwave Suite 2019 and HFSSv15 full-wave simulators are used.

It is necessary to mention the numerical model and the type of analysis performed for full-wave simulations by CST software is time domain solver with mesh type of hexahedral and accuracy -40 dB model. Also, the numerical model of analysis by HFSS software is the Frequency Domain. Some other properties of the used dielectric are: Thermal

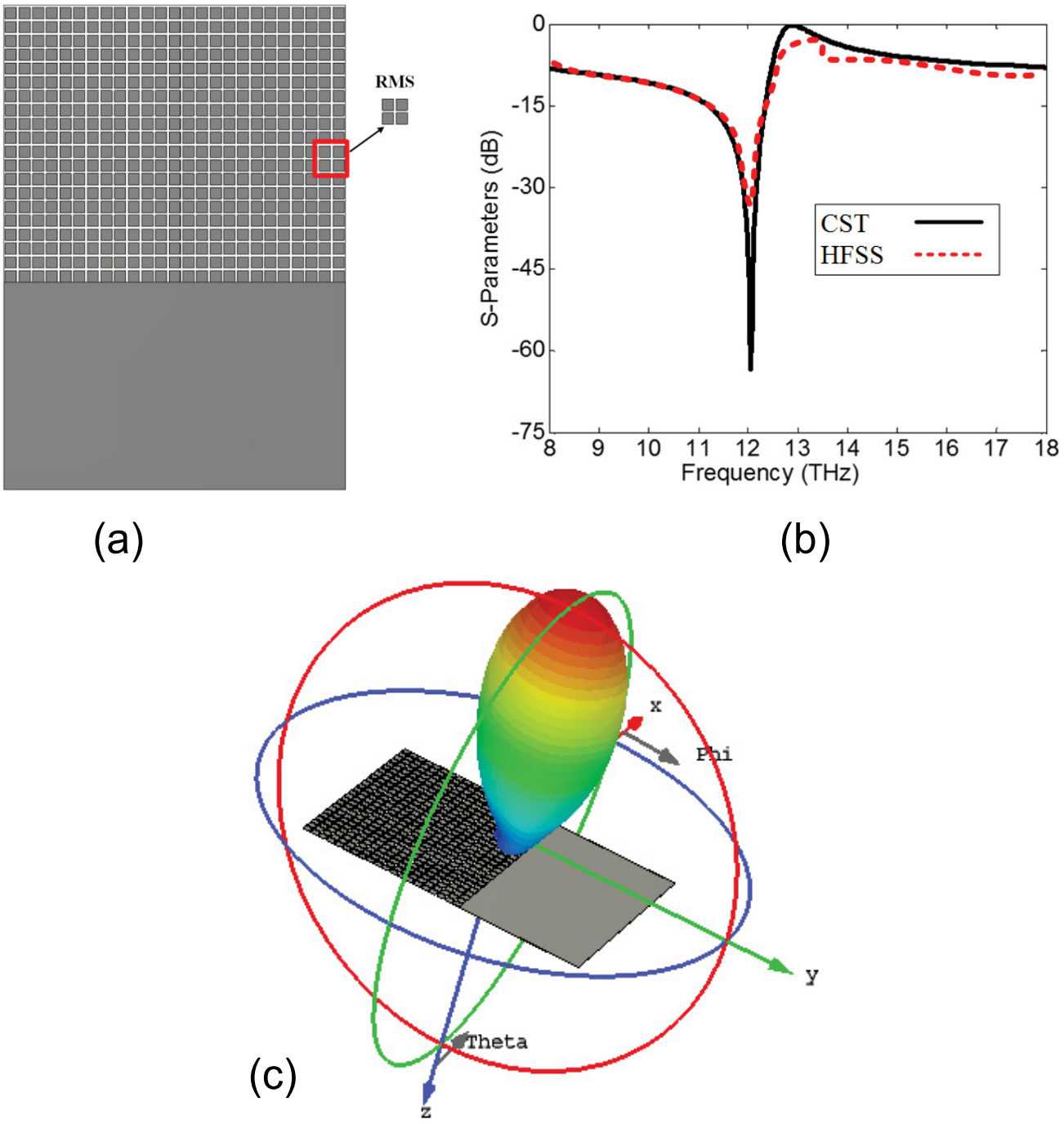

Figure 1: a) Proposed RMS; b) S_{21} parameter; c) 3D radiation pattern of the proposed RMS.

coefficient is -121 (ppm/C), volume resistivity and surface resistivity are 3 × 109 (Mohm cm) and 4 × 109 (Mohm), respectively, and specific heat is 0.93 (J/g/K). Also, all the simulations are done by an Intel Core i5 2.30 GHz processor and 12 GB of memory. The average time taken to the simulation by CST and HFSS are 89 and 94 minutes, respectively.

At first, an RMS cell is selected. By placing it on the *xy* plane, the perfect magnetic conductor (PMC) boundary condition on the *xy* planes is also used, as well as the perfect electric conductor (PEC) boundary condition on the *yz* plane. Finally, by applying a plane wave with horizontal polarization along the x-axis, simulation is performed. The result of the S_{21} parameter of this structure is presented in Figure 1b. It is observed that a transmission-zero (TZ) is generated at 12 THz. This is an obvious function for metasurface and metamaterial structures. Because these structures behave like an *LC* circuit that can model a band stop filter [16]. By applying the mentioned plane wave, a three-dimension-

al (3D) radiation pattern is obtained. This feature, shown in Figure 1c, proves that the direction of the beam, or the improvement of the directivity at 12 THz, is clearly visible. The directive of the radiating pattern, instead of omnidirectional, is a compelling reason for the ability to increase the antenna gain.

It is necessary to mention the proposed RMSs, like dielectric lenses, can concentrate electromagnetic waves which generate from dipole antenna. RMS environment also prevents electromagnetic fields from spreading in undesirable directions due to their absorbency. Therefore, directivity and gain of the antenna will increase. On the other hand, in [18] written by the authors, the phase of electromagnetic fields is plotted for different permeability in the metamaterial medium. It is clear that the electromagnetic fields propagate at a higher phase velocity inside the metamaterial medium. Therefore, the antenna directivity and gain will improve. So, by using the RMS layer at the top of the microstrip dipole antenna, it can be claimed that the gain can be increased.

Antenna design and results

The configuration of a conventional microstrip dipole antenna which presented in [17] is shown in Figure 2. This antenna comprised of an L-shaped resonator for end-fire electromagnetic waves propagation and a Rogers RT6010LM dielectric substrate with relative permittivity of 10.7, tan δ = 0.0023, and heights 1 mm and 5 mm.

Figure 3a shows the return loss (S_{11}) of this antenna. This parameter is one of the most important characteristics of an antenna. Assumption S_{11} <

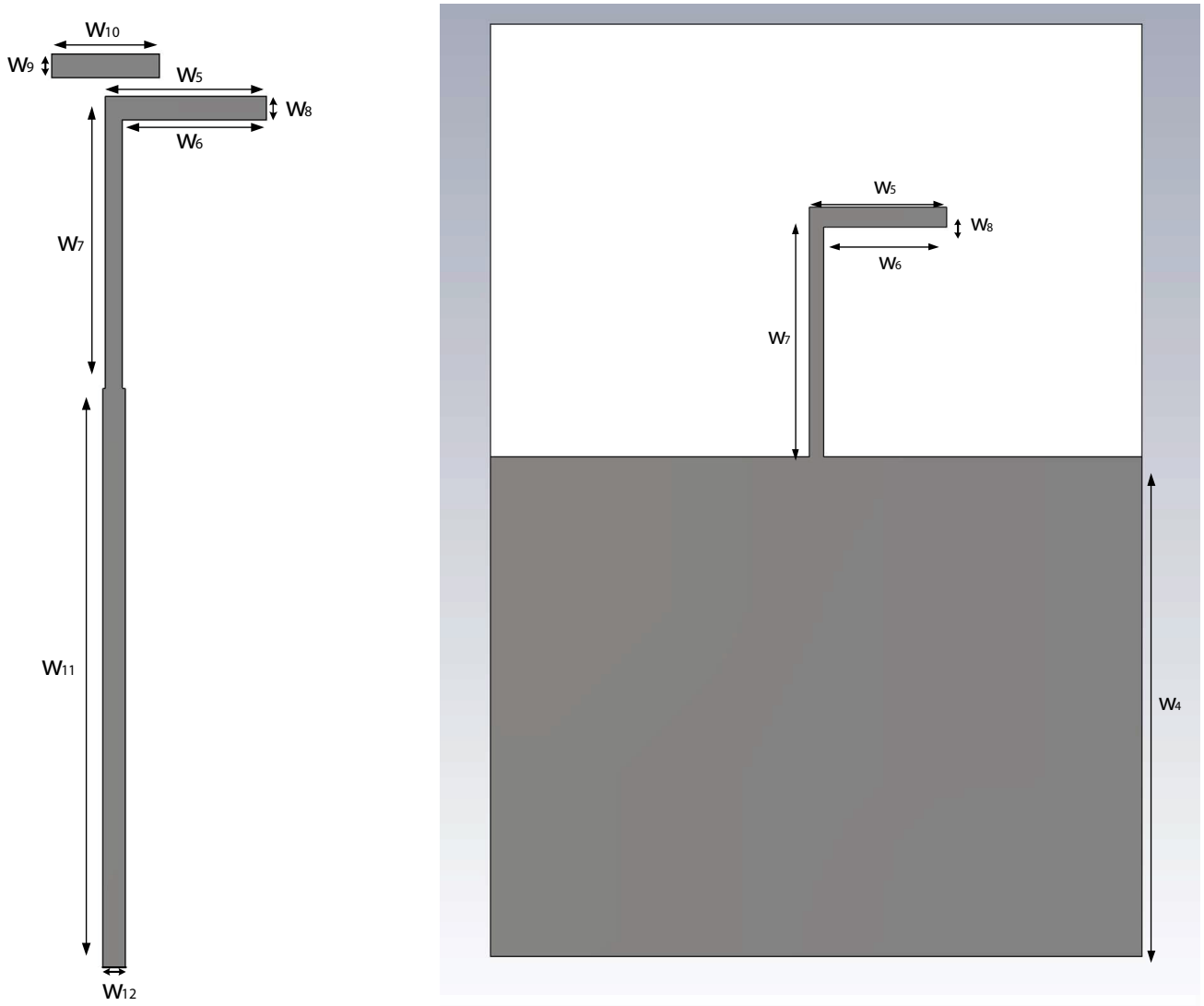

Figure 2: Conventional single layer microstrip dipole antenna.

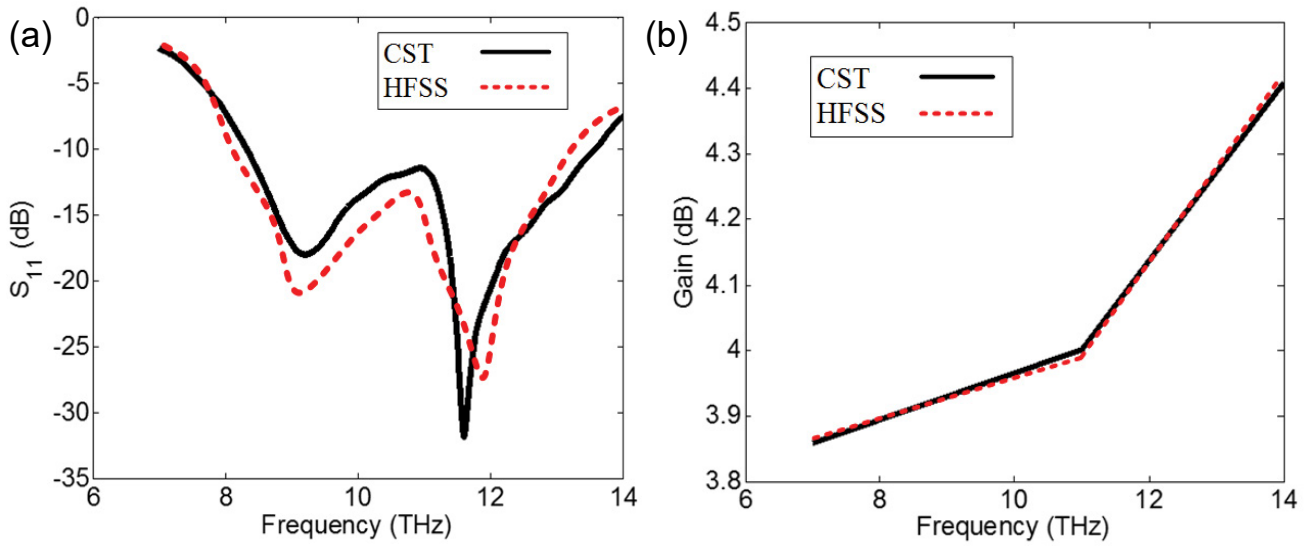

Figure 3: a) Return loss; b) Gain of the conventional dipole antenna.

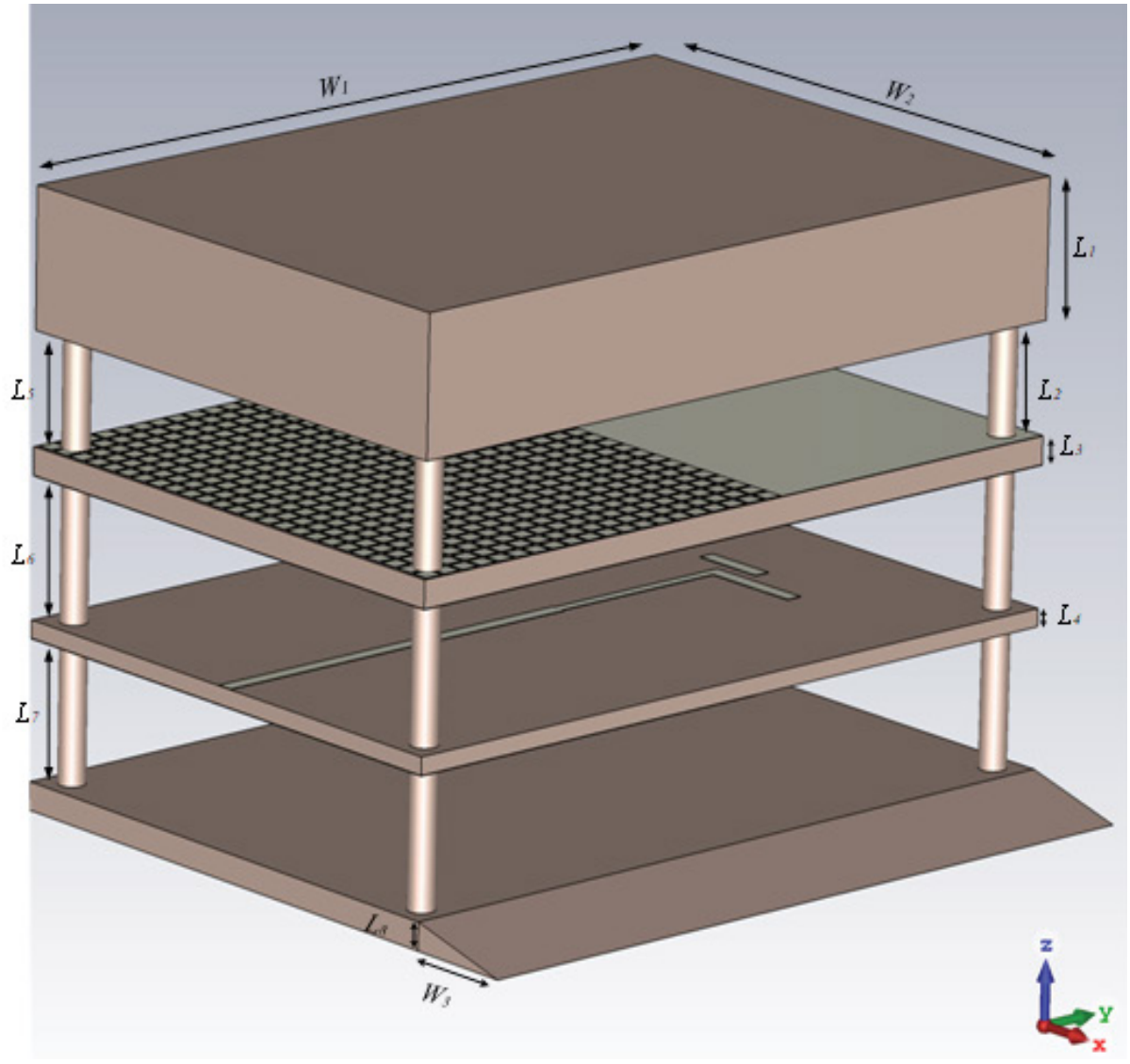

Figure 4: Configuration of the proposed terahertz high-gain antenna.

-10 dB is a reasonable assumption for determining antenna bandwidth. Therefore, in the frequency ranges where the above condition is met, the return loss of the antenna input signal is less than 0.1 of its maximum value. Therefore, this frequency range is referred to as antenna bandwidth. So, it is observed that the bandwidth is equal to 5.5 THz (8-13.5 THz). Figure 3b also shows the realized gain of this antenna. It can be seen that the average gain in the mention frequencies is about 4.2 dB by tow software. Now our goal is to improve the gain of this antenna by using the RMS layer introduced in the previous part.

Figure 4 shows the final configuration of the proposed antenna. It is observed that this antenna has 4 layers. The layer made up of the proposed RMS medium is located at the top of the dipole antenna. At the bottom of the antenna, a Rogers RT6010LM dielectric with a height of 5 mm is used. In addition to creating strength, this section has improved the gain by more than 0.65 dB. In the layer above the RMS layer, another Rogers RT6010LM dielectric layer is placed to increase the gain by 0.45 dB. It should be noted that with the increase in the number of layers at the bottom and top of this antenna, from 3 to 12 layers, the gain enhancement is only 1 dB. So, the same 4 layers will be used to prevent excessive dimensions. Therefore, the upper and lower layers have improved the gain by a total of 1.1 dB. But the RMS layer alone has increased the antenna's gain by more than 9.5 dB. It should be noted that 8 plastic bases have been used to connect the layers. These bases do not have a detrimental effect on the antenna's radiation patterns. All dimensions of this antenna, as well as the conventional antenna are: W_1 = 28, W_2 = 20, W_3 = 4, W_4 = 16, W_5 = 4.23, W_6 = 3.7858, W_7 = 7.5, W_8 = 0.6, W_9 = 0.6, W_{10} = 2.84, W_{11} = 15, W_{12} = 0.5923, L_1 = 5, L_2 = 4, L_3 = 1, L_4 = 0.64, L_5 = 4.018, L_6 = 5, L_7 = 4.982, and L_8 = 1 (all in millimeters).

The scattering parameters (S-parameter) of the proposed antenna are shown in Figure 5a. Assuming S_{11} < -10 dB, the bandwidth is equal to 5 THz (8-13 THz). The gain of the proposed antenna is shown in Figure 5b. It is observed that at 12 THz, a maximum gain of 14.7 dB is obtained. It should be noted that these results have also been obtained by both CST and HFSS. There is a good fit between the results of both simulators.

In the following, several parametric reports will be presented the selected optimal choices will be introduced. In the first report, the effect of the proposed RMS unit-cell dimensions on the TZ location was investigated. Figure 6 shows the TZ frequency for different RMS dimensions. It is observed that with increasing dimensions from 0.2 mm^2 to 0.5 mm^2, the TZ frequency decreases from 14.36 THz to 9.1 THz. Therefore, for resonance at 12 THz, the value of 0.36 mm^2 will be an optimal choice. It should be noted that this phenomenon is a natural issue in the design of microstrip structures. Because the effective length of a structure is inversely related to the resonant frequency. Therefore, it is clear that with increasing dimensions, the resonance frequency decreases and vice versa.

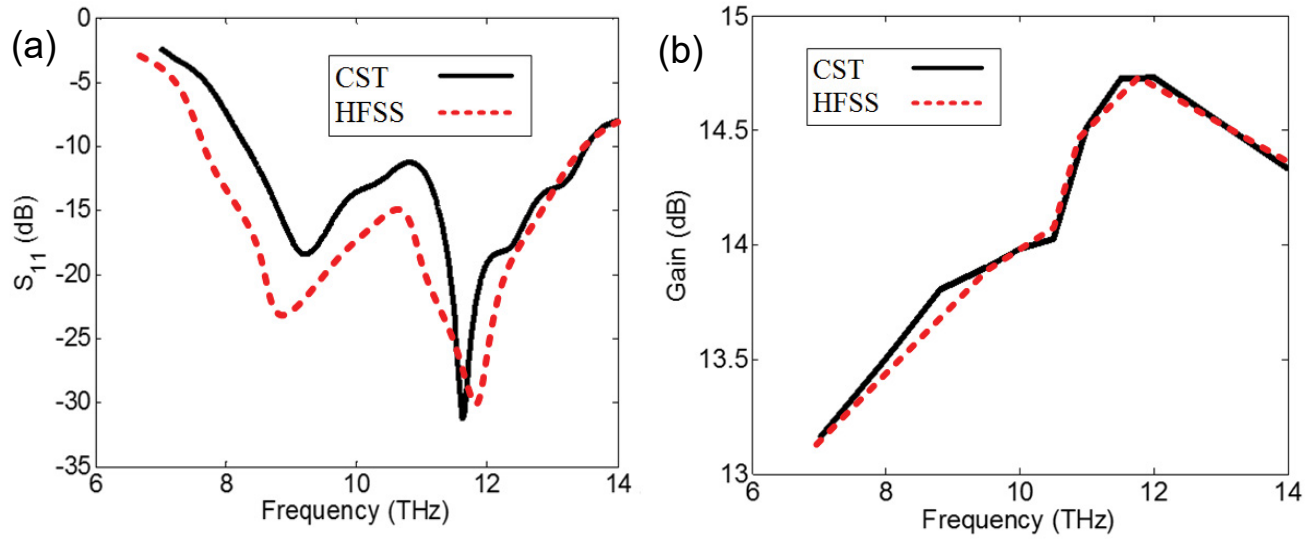

Figure 5: a) Return loss; b) Gain of the proposed terahertz antenna.

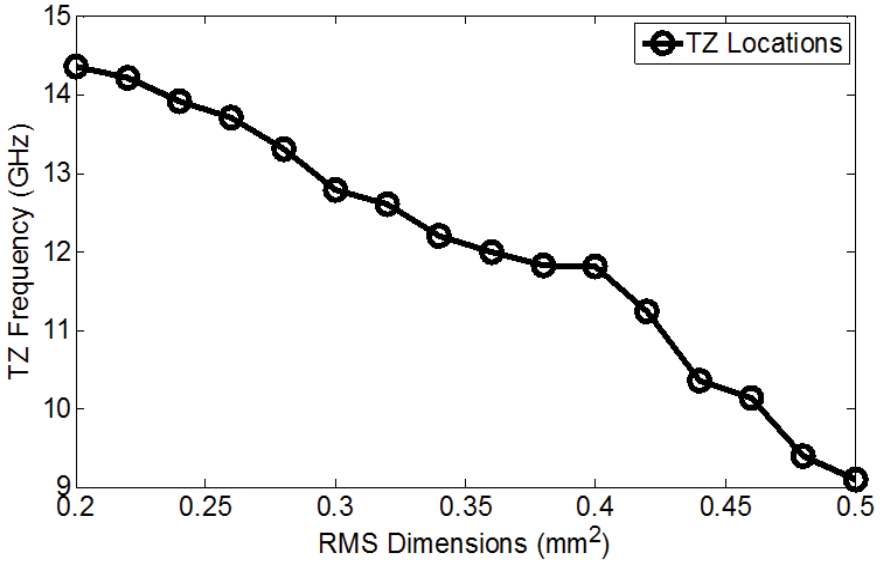

Figure 6: TZ frequency changes for different RMS dimensions.

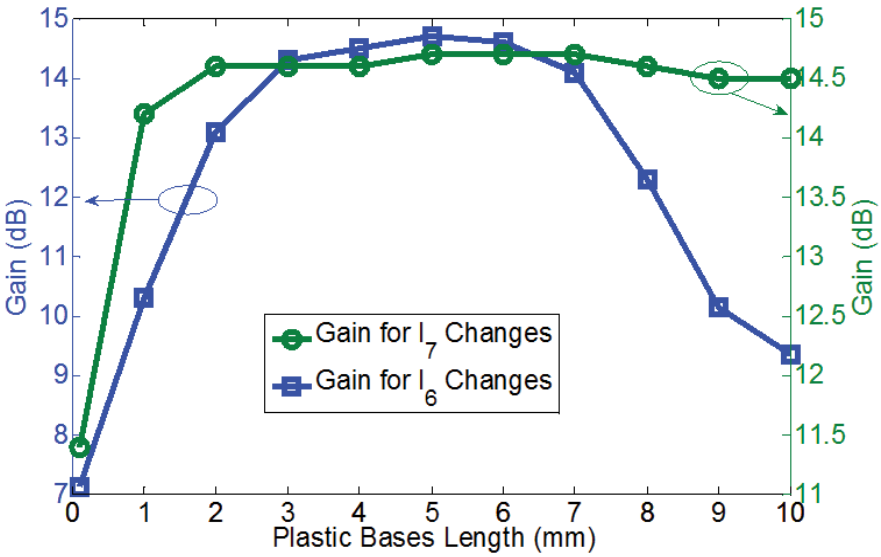

Figure 7: Antenna gain for different values of the L_6 and L_7 parameters.

In the second report, the effect of the heights of the plastic bases (L_6 and L_7) on the gain of the proposed antenna at 12 THz is investigated. Figure 7 shows the proposed antenna gain for different values of the L_6 and L_7 parameters. It is important to note that when the length L_6 is too small ($L_6 < 0.2$ mm), the antenna gain greatly decreases. The same is true for the L_7 parameter. Also, by increasing the distance of the RMS layer from the dipole antenna ($L_6 > 6$ mm), the gain will decrease too. The reason for the decrease in the gain in the first case is the creation of a very strong electromagnetic field coupling and destructive wave interference between the dipole antenna and the RMS layer, which drastically reduces the gain and the radiation efficiency. The reason for the decrease in the gain in the second case is that by increasing the distance between the RMS layer and the dipole antenna reduces the constructive interference between electromagnetic waves [29]. Therefore, there will always be an optimal distance in which there is the most constructive interference and the antenna gain will be maximized [29]. So, the optimal distance between the antenna and the RMS layer is $L_6 = 5$ mm. Also, according to Figure 7, the optimal value for the L_7 parameter is about 4.982 mm. Given these values, the maximum gain at 12 THz will be 14.7 dB.

Then, for $L_6 = 2$ mm, $L_6 = 5$ mm, and $L_6 = 8$ mm

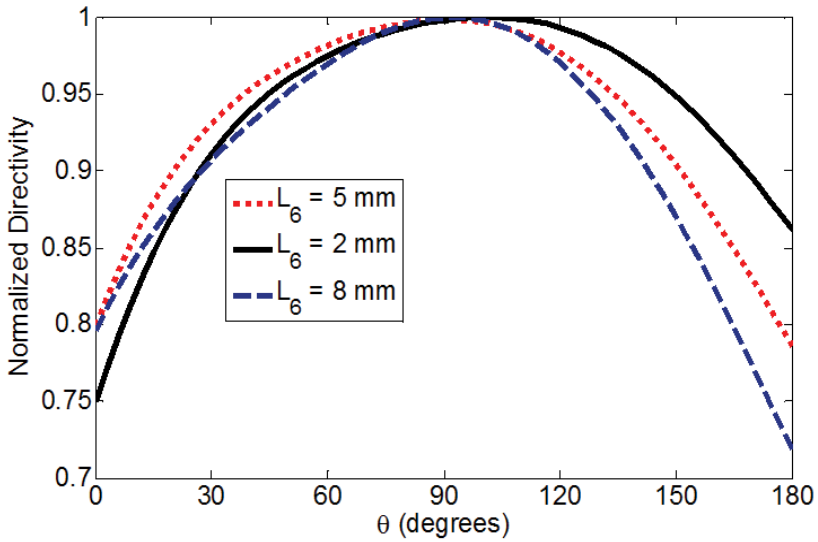

Figure 8: Cartesian radiation patterns of the proposed antenna at 12 THz.

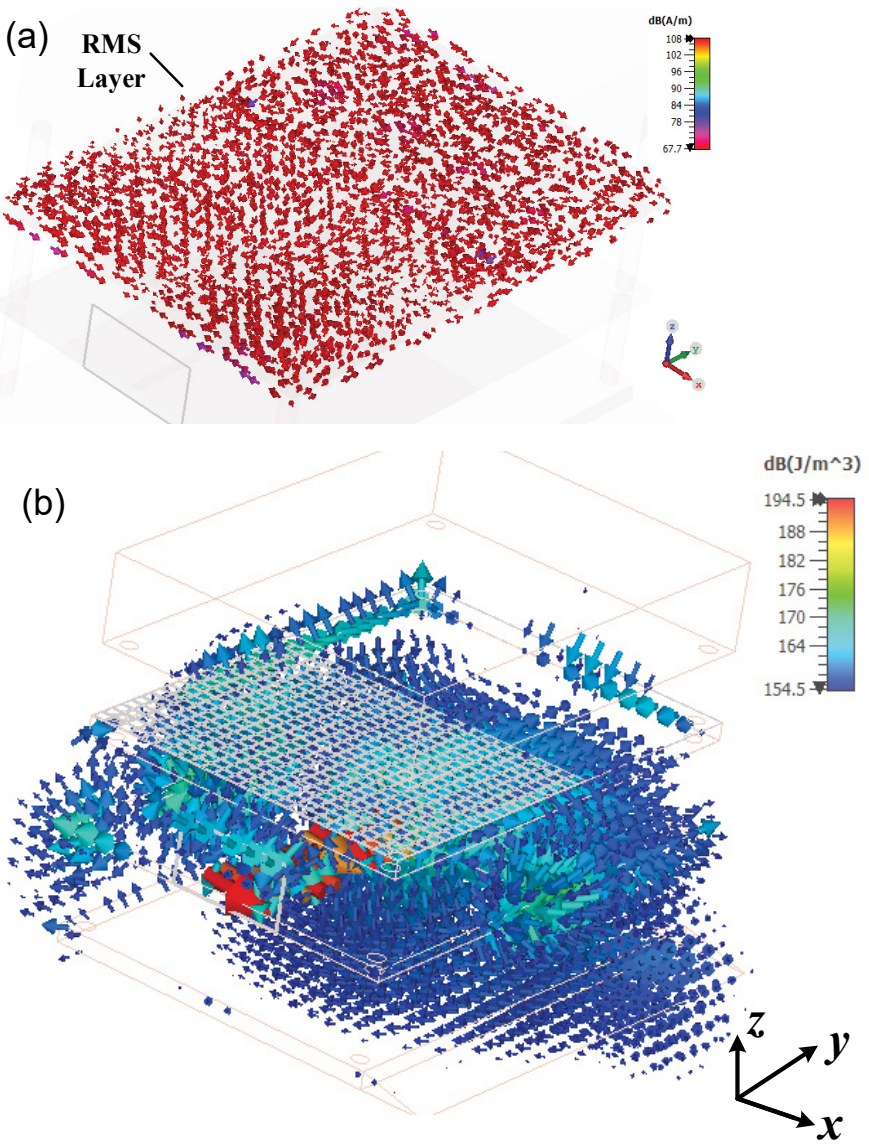

Figure 9: a) The surface current density; b) Power flow distribution of the proposed antenna at 12 THz.

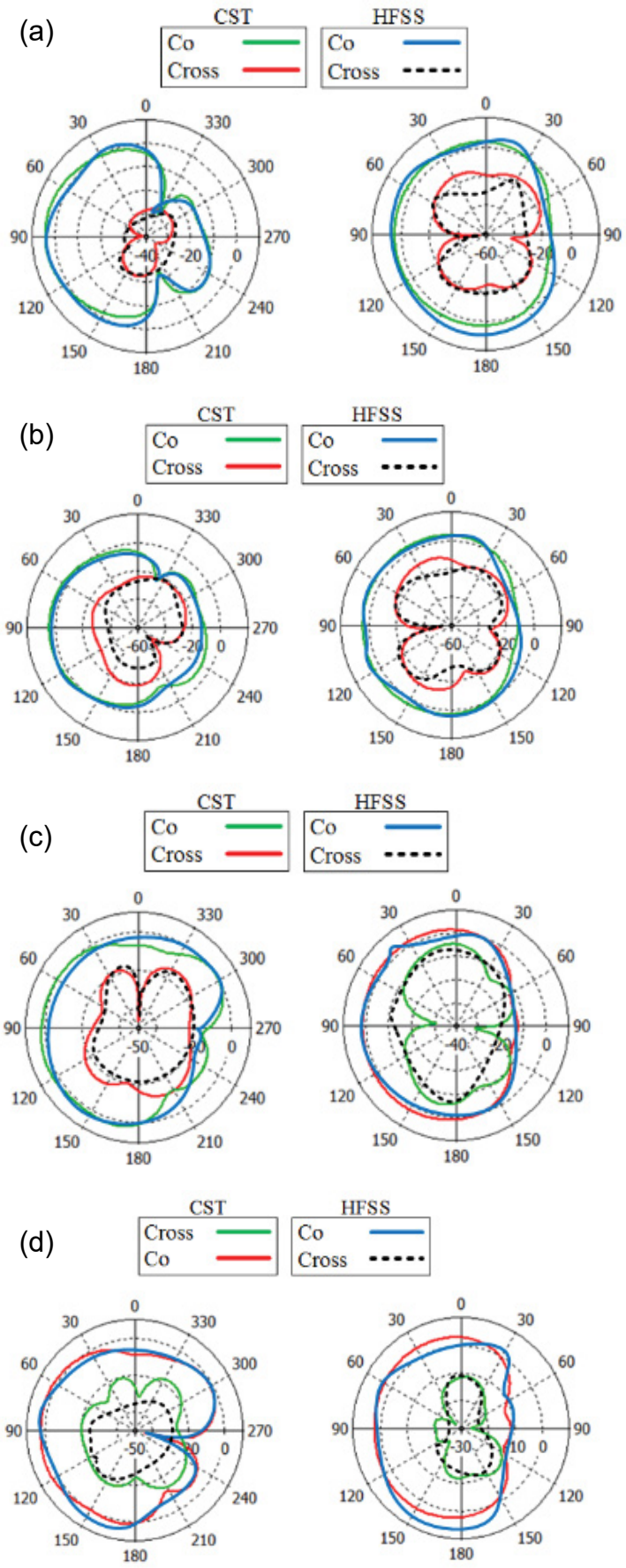

Figure 10: Simulated polar radiation patterns of the proposed terahertz high-gain antenna at several frequencies on both the *E*- and *H*-planes by CST and HFSS simulators: a) 9 THz; b) 10 THz; c) 11 THz; d) 12 THz.

Table 1: Comparison between the proposed terahertz antenna and other works.

Ref.	Technique	Center Frequency (THz)	Peak of Gain (dB/dBi)	Gain Enhancement (dB/dBi)
[4]	Graphene	5	12.8 dBi	2.11 dBi
[12]	Metamaterial	5.4	4.14 dB	---
[13]	Meander-line/defected ground	4.24	7.54 dBi	---
This work	RMS	12	14.7 dB	10.6 dB

(as several examples), the cartesian radiation patterns of the proposed terahertz antenna at 12 THz is calculated. These patterns, shown in Figure 8 are on the *E*-plane. In these three cases, the radiation patterns are almost identical. Therefore, changes in the dimensions of the plastic bases will not have a detrimental effect on the radiation patterns.

Figure 9a shows the surface current density at a 12 THz for the RMS layer. As mentioned in Section II, this layer acts as a parasitic medium. Therefore, by concentrating the electromagnetic waves, it increases the gain and directivity of the proposed antenna. Figure 9b also shows the power flow distribution at 12 THz. It can be seen that most of the power is concentrated in the RMS layer.

Figure 10 shows the polar radiation patterns of the proposed terahertz antenna for frequencies of 9, 10, 11, and 12 THz on both the *E*- and *H*-planes by both CST and HFSS simulators. Note that in each case, both the co- and cross-polarization attributes are reported. The shapes on the left are for the *E*-plane and the shapes on the right are for the *H*-plane. It can be seen that there is an acceptable fit between the results of both software. Also, comparing Figure 8 and Figure 10, it is observed that the dimensions of the plastic bases do not have a destructive effect on the radiation patterns of the antenna. Although there are differences between the results of both simulators, these differences are acceptable for these “qualitative” charts. The reason for making more differences in this section compared to S-parameters, the existence of the creation of radiation air boxes with different dimensions, due to different numerical methods in problem solving.

Finally, in order to provide a comparison between the performance of the proposed antenna and the other antennas presented in the articles, Table 1 has been compiled. It is observed that the proposed antenna has favorable conditions. Among the positive and valuable points of the proposed antenna in this work, we can mention the simplicity of the design, the use of only one method to increase the gain, and also the use of microstrip structures in the design at terahertz frequencies. Another great advantage of this antenna is its very good gain. A gain rate of more than 10.5 dB proves this claim. However, using methods such as metamaterial and graphene structures, the gain rate has improved by about 2 dBi.

Conclusion

In this paper, a high-gain multi-layer antenna was designed to be used in terahertz communication systems with a frequency range of 8-13 THz. In this design, using the proposed RMS medium, the gain equal to 14.7 dB at 12 THz was obtained. However, the gain of the conventional of this antenna is equal to 4.1 dB. The benefits of this antenna include design innovation, wide bandwidth, and high realized gain.

References

1. F Khajeh-Khalili, F Haghshenas, A Shahriari (2020) Wearable dual-band antenna with harmonic suppression for application in medical communication systems. AEU-International Journal of Electronics and Communications 126: 1-8.
2. A Kishk (2014) Advancement in microstrip antennas with recent applications. InTech, Rijeka, Croatia.
3. AT Hassan, AA Kishk (2020) Efficient procedure to design large finite array and its feeding network with examples of ME-dipole array and microstrip ridge gap waveguide feed. IEEE Transactions on Antennas and Propagation 68: 4560-4570.
4. M Roshanaei, H Karami, P Dehkhoda, H Esfahani, F Dabir (2020) A highly directive graphene antenna embedded inside a Fabry-Perot cavity in terahertz regime. Super Lattices and Microstructures 117: 356-363.
5. A Dadgarpour, MS Sorkherizi, AA Kishk (2017)

High-efficient circularly polarized magnetoelectric dipole antenna for 5G applications using dual-polarized split-ring resonator lens. IEEE Transactions on Antennas and Propagation 65: 4263-4267.

6. WEI Liu, ZN Chen, X Qing (2020) Miniature wideband non-uniform metasurface antenna using equivalent circuit model. IEEE Transactions on Antennas and Propagation 68: 5652-5657.

7. A Verma, AK Singh, N Srivastava, S Patil, BK Kanaujia (2020) Hexagonal ring electromagnetic band gap-based slot antenna for circular polarization and performance enhancement. Microwave and Optical Technology Letters 62: 2576-2587.

8. H Aliakbari, M Mosalanejad, C Soens, GAE Vandenbosch, BK Lau (2019) Wideband SIW-based low-cost multilayer slot antenna array for E-band applications. IEEE Transactions on Components, Packaging and Manufacturing Technology 9: 1568-1575.

9. MB Kakhki, A Dadgarpour, AR Sebak, TA Denidni (2020) Twenty-eight-gigahertz beam-switching ridge gap dielectric resonator antenna based on FSS for 5G applications. IET Microwaves, Antennas & Propagation 14: 397-401.

10. AJ Alazemi, HH Yang, GM Rebeiz (2016) Double bow-tie slot antennas for wideband millimeter-wave and terahertz applications. IEEE Transactions on Terahertz Science and Technology 6: 682-689.

11. S Singha, Jaiverdhan (2020) Hexagonal fractal antenna for super wideband terahertz applications. Optik 206: 1-7.

12. K Bhattacharyyaa, S Goswamib, K Sarmahb, S Baruah (2019) A linear-scaling technique for designing a THz antenna from a GHz microstrip antenna or slot antenna. Optik 199: 1-8.

13. S Ghosh, S Das, D Samantaray, S Bhattacharyya (2020) Meander-line-based defected ground microstrip antenna slotted with split-ring resonator for terahertz range. Engineering Reports 2: 1-9.

14. F Khajeh-Khalili, MA Honarvar (2018) Novel tunable peace logo planar metamaterial unit-cell for millimeter-wave applications. ETRI Journal 40: 389-395.

15. F Khajeh-Khalili, MA Honarvar, A Dadgarpour (2018) High-gain bow-tie antenna using array of two-sided planar metamaterial loading for H-band applications. International Journal of RF and Microwave Computer-Aided Engineering 28: 1-7.

16. F Khajeh-Khalili, MA Honarvar, A Dadgarpour, BS Virdee, TA Denidni (2019) Compact tri-band Wilkinson power divider based on metamaterial structure for Bluetooth, WiMAX, and WLAN applications. Journal of Electromagnetic Waves and Applications 33: 707-721.

17. F Khajeh-Khalili, MA Honarvar, M Naser-Moghadasi, M Dolatshahi (2020) Gain enhancement and mutual coupling reduction of multiple-intput multiple-output antenna for millimeter-wave applications using two types of novel metamaterial structures. International Journal of RF and Microwave Computer-Aided Engineering 30: 1-9.

18. MA Raghvendra, K Chaudhary (2020) Dual-layer and dual-polarized metamaterial inspired antenna using circular-complementary split ring resonator mushroom and metasurface for wireless applications. AEU-International Journal of Electronics and Communications 113: 1-48.

19. VG Veselago (1968) The electrodynamics of substances with simultaneously negative values of ε and μ. Soviet Physics Uspekhi 10: 509-514.

20. DR Smith, S Schultz, P Markoš, CM Soukoulis (2002) Determination of effective permittivity and permeability of metamaterials from reflection and transmission coefficients. Physical Review B 65: 1-5.

21. Y Shen, J Zhang, Y Pang, L Zheng, J Wang, et al. (2018) Thermally tunable ultra-wideband metamaterial absorbers based on three-dimensional water-substrate construction. Nature Scientific Reports 8: 1-10.

22. P Jin, RW Ziolkowski (2010) Broadband, efficient, electrically small metamaterial-inspired antennas facilitated by active near-field resonant parasitic elements. IEEE Transactions on Antennas and Propagation 58: 318-327.

23. A Dadgarpour, N Bayat-Makou, MA Antoniades, AA Kishk, A Sebak (2020) A dual-polarized magnetoelectric dipole array based on printed ridge gap waveguide with dual-polarized split-ring resonator lens. IEEE Transactions on Antennas and Propagation 68: 3578-3585.

24. F Yang, Y Rahmat-Samii (2003) Microstrip antennas integrated with electromagnetic band-gap (EBG) structures: A low mutual coupling design for array applications. IEEE Transactions on Antennas and Propagation 51: 2936-2946.

25. J Wang, H Wong, Z Ji, Y Wu (2019) Broadband CPW-fed aperture coupled metasurface antenna. IEEE Antennas and Wireless Propagation Letters 18: 517-520.

26. J Guo, F Liu, L Zhao, Y Yin, GL Huang, et al. (2019) Meta-surface antenna array decoupling designs for two linear polarized antennas coupled in H-plane and E-plane. IEEE Access 7: 100442-100452.

Citation: Khajeh-Khalili F, Dohni-Zadeh Y (2020) High-Gain Multi-Layer Antenna Using Metasurface for Application in Terahertz Communication Systems. Int J Electron Device Phys 4:007

27.T Li, ZN Chen (2018) A dual band metasurface antenna using characteristic mode analysis. IEEE Transactions on Antennas and Propagation 66: 5620-5624.

28.J Hu, GQ Luo, ZC Hao (2017) A wideband quad-polarization reconfigurable metasurface antenna. IEEE Access 6: 6130-6137.

29.F Khajeh-Khalili, MA Honarvar (2016) A design of triple lines Wilkinson power divider for application in wireless communication systems. Journal of Electromagnetic Waves and Applications 30: 2110-2124.

DOI: 10.35840/2631-5041/1707

Citation: Khajeh-Khalili F, Dohni-Zadeh Y (2020) High-Gain Multi-Layer Antenna Using Metasurface for Application in Terahertz Communication Systems. Int J Electron Device Phys 4:007